1993 SCA Conference Paper Number 9309

THE INFLUENCE OF POROSITY, PERMEABILITY, TORTUOSITY, WETTABILITY AND MERCURY POROSIMETRY PROPERTIES ON LIMESTONE WATERFLOOD RESIDUAL OIL SATURATION

Olubunmi O. Owolabi and Robert W. Watson
Petroleum and Natural Gas Engineering, The Pennsylvania State University

ABSTRACT

This paper deals with experimental and theoretical studies to investigate certain rock/pore properties of limestone rocks that previously have not been fully investigated and correlated to waterflood residual oil saturation. Apart from porosity and permeability, the other rock/pore properties investigated are tortuosity, formation resistivity factor, wettability index, pore intrusion volume, pore surface area, pore-throat diameter, pore skeletal density and recovery efficiency.

To accomplish the above stated objective, waterflood experiments were conducted on 16 limestone linear-cores ranging in length from 40.0 cm to 45.7 cm in length and diameter from 3.76 to 3.89 cm. The cores were flooded at different rates depending on their scaling coefficient (product of core length in cm, water velocity in cm/min and water viscosity in cp), which was kept at an approximately constant value of 5.0 The limestone rocks investigated were mainly from the Indiana limestone units which were formed in shallow inland sea during Mississippian time.

Thirty-two core plugs were extracted from each of the waterflooded cores from positions perpendicular to the flood plane (for a total of 512 core plugs) and further analyzed by conducting the wettability and mercury porosimetry experiments. The cores investigated were all water-wet and the results of the mercury porosimetry experiments suggested that bimodal pore-size distributions are characteristic of the limestone core samples.

The results of these tests are presented and incorporated into empirical models for the prediction of residual oil saturation at breakthrough and at floodout, from waterflooding for limestone reservoirs. The models indicated that residual oil saturation is strongly correlated to porosity, permeability, tortuosity, formation resistivity factor, irreducible water saturation, pore intrusion volume, skeletal density and mercury recovery efficiency.

References and illustrations at the end of paper.

INTRODUCTION

A good knowledge of the basic properties of the reservoir rocks, is one of the requirements for gaining a better understanding of waterflood performance. This study is aimed at correlating rock-pore characteristics to residual oil saturation from limestone rocks and incorporating these properties into empirical models for predicting residual oil saturation. For that reason, this report deals with the analyses and interpretation of experimental data collected from core floods and correlated against measurements of porosity, permeability, tortuosity, wettability index, mercury porosimetry properties and irreducible water saturation.

The most important component of reservoir characterization is the description of the pore systems, which is one of the factors that control the production potential of the reservoir. Pore systems are studied by a family of methods called petrophysical analysis; one of these methods is mercury porosimetry (Kopaska-Merkel and Friedman, 1989). In this method, mercury is injected into the pore system of a sample under controlled conditions, to produce capillary pressure curves. The properties of interest from the mercury porosimetry include total mercury intrusion volume, pore surface area, specific surface area, average pore diameter, skeletal density, apparent porosity, residual mercury saturation and mercury recovery efficiency.

Empirical model based on data obtained from waterflood, wettability and mercury porosimetry laboratory experiments were developed for the predictions of residual oil saturation at both the breakthrough and floodout conditions. Furthermore, the model was developed for limestones using unfired linear Indiana limestone cores.

EXPERIMENTAL PROCEDURE

Figure 1 shows a schematic of the experimental procedure. As indicated in the figure, for the core-floods, linear cores were utilized and flow of the injected oil or brine was parallel to the bedding plane. Core plugs were extracted from each of the waterflooded cores. The core plugs were later used for the wettability and mercury porosimetry tests.

Waterflood Experiments

The experimental apparatus used for this investigation was a fully automatic core-flooding station developed by Core Test Systems, Mountain View, California. This system permitted the simulation of both reservoir temperature and overburden pressure. Sixteen Indiana limestone corefloods were performed. The limestone cores used in these experiments ranged from 40.00 cm to 45.72 cm in length and from 3.76 cm to 3.89 cm in diameter.

The experimental procedure required that the core be evacuated to a pressure of 50-100 microns of mercury. After this was achieved, the core was then saturated with brine.

Tortuosity was measured by recording the amount of time required for the injected brine to traverse from the core inlet to the outlet face. The pore volume was determined by measuring the amount of brine used to completely saturate the core. After the core was saturated with brine, the absolute permeability was determined. The core was then subjected to the drainage and imbibition processes of flooding to determine properties such as irreducible water saturation, residual oil saturation at breakthrough, and residual oil saturation at floodout). The brine used consisted of 1.5% by weight sodium chloride, 0.3% by weight formalin (37% by volume formaldehyde), and 98.2% by weight distilled water. The formalin was used to preserve the brine and prevent bacterial growth. The non-wetting phase was a binary system containing 70% by volume Blandol and 30% by volume of Soltrol 160. This combination was selected to yield a viscosity of 10.0 cp at 35°C. The physical properties of the fluids are shown in Table 1 and those of the cores are as shown in Table 2. The scaling coefficients were maintained at approximately 5.0 cm^2.cp/min, in order to prevent end-effects.

After the completion of the waterflood experiments and in readiness for the wettability and mercury porosimetry experiments, core plugs were extracted from the waterflooded cores. Thirty-two core plugs were taken from each of the 16 Indiana limestone cores, for a total of 512 limestone core plugs. The core plugs were drilled perpendicular to the bedding planes on each limestone core, using a diamond core bit with water as the coolant and lubricant. Each core plug was identified by a sample number, using blue color wax-base pencil. On the average, the extracted core plugs were 1.3 cm in diameter and 1.7 cm long. The core plugs were cleaned prior to performing the wettability and mercury porosimetry tests by using the technique developed by Texaco Research Laboratory (Owolabi, 1993).

Wettability Experiments

Wettability is a major factor controlling the location, flow and distribution of fluids in a reservoir. The term is generally used to describe the ability of a fluid to wet a solid surface in the presence of the second fluid. The Amott-Harvey (Amott, 1959) method was used to measure the average wettability of the core plugs which were extracted from the waterflooded cores. The method is based on the fact that the wetting fluid will generally imbibe spontaneously into the core, thereby displacing the non-wetting phase. In determining the wettability index, the ratio of spontaneous imbibition to forced imbibition is utilized to reduce the influence of other factors, such as relative permeability, viscosity, and the initial saturation of the rock because only the surface forces are changed (Anderson, 1986). A description of the experimental procedure is summarized as follows:

1. Centrifuge core plug under brine.
2. Centrifuge under reservoir crude.

   Carefully weigh the core plug at the end of step 2.
3. Submerge in brine for 20 hours and find "A".

   The value of "A" is equal to the weight of the core plug at the end of step 3 less the weight of the core plug at the end step 2.
4. Centrifuge under brine and find "B".

   The value of "B" is equal to the weight of the core plug at the end of step 4 less the weight of the core plug at the end step 3.

5. Submerge in reservoir crude oil for 20 hours and find "C".

   The value of "C" is equal to the weight of the core plug at the end of step 5 less the weight of the core plug at the end step 4.

6. Centrifuge under crude oil and find "D".

   The value of "D" is equal to the weight of the core plug at the end of step 6 less the weight of the core plug at the end step 5.

7. Determine relative displacement (wettability) index as:

$$WI = \left[\frac{A}{A+B}\right] - \left[\frac{C}{C+D}\right] \quad (1)$$

The samples are centrifuged for 1 hour with the speed control knob of the centrifuge set at between one-half to full speed or at about 1500 RPM.

For the Amott-Harvey method, water-wet range is from +0.3 to +1.0, the intermediate range is from -0.3 to +0.3 and the oil-wet range is from -0.3 to -1.0 (Cuiec, 1987). The intermediates are further broken down to a range of +0.1 to +0.3 for slightly water-wet, -0.1 to +0.1 for neutral and -0.1 to -0.3 for slightly oil-wet.

Mercury Porosimetry Experiments

The experiments were carried out on a mercury porosimetry (Pore Sizer Model Autopore II 9220) supplied by Micromeritics, Norcross, Georgia. To embark on the tests, the samples were weighed and installed in penetrometers individually. Four samples in penetrometers were installed in the low-pressure ports at a time and evacuated simultaneously in low pressure ports until a stabilized pressure of about 50 μm was obtained. Mercury was then allowed to fill the penetrometers and low-pressure tests were performed by permitting dry air to be admitted in discrete increments from 1.5 psia to 14 psia (about atmospheric pressure).

At the conclusion of the low pressure runs, the penetrometers containing mercury and samples were weighed and two of them were installed in the high-pressure chambers at a time. The high-pressure runs could be performed at specific values from 14 to 60,000 psia (air-mercury) by raising the pressure incrementally and allowing equilibration at each increment. With each increment of pressure, smaller pore throats were invaded by mercury. For this present study, the maximum pressure was limited to 11,000 psia, because the amount of mercury intrusion above this pressure is negligible for the types of samples being investigated.

Pore size information are obtained from mercury intrusion (drainage) curves based on the assumption of a cylindrical pore configuration. It is assumed that mercury is the non-wetting

phase which displaces completely the wetting phase (mercury vapor or air) in the rock samples. The extrusion (imbibition) curves are obtained by releasing pressure and recording equilibrated values and taking readings at successively lower pressures (Ghosh and Friedman, 1989).

RESULTS AND DISCUSSION

Sixteen sets of waterflooding displacement tests were conducted in Indiana limestone cores of varying lengths. Oil was displaced from the cores by brine at an overburden pressure of 500 psig and at a fixed temperature of 35°C. Brine was injected at rates varying from 1.23 to 1.48 cc/min, depending on the diameter and length of the core being tested.

Most of the figures in this report are fitted with simple regressions and the goodness of the correlation analyzed on the figures. The simple regressions were performed using MINITAB statistical computer package (Ryan et al, 1985). Statistical significance of the simple regression correlation were analyzed at significance levels, α, of 0.001, 0.005, 0.01, 0.05 and 0.1. These correspond to F-test statistic values of 17.27, 11.13, 8.90, 4.61 and 3.11, respectively (Neter et al, 1990).

The permeability, tortuosity, and formation resistivity factor versus porosity for the 16 core samples are plotted in Fig. 2, 3 and 4, respectively. The plots show that as porosity increases, permeability also increases, but tortuosity and formation resistivity factor decrease. These trends exhibited by the rock-pore characteristics investigated are comparable to the published trends in the literature (Amyx et al, 1960). The tortuosity versus porosity relationship is statistically significant at $\alpha = 0.005$ level and that of formation resistivity factor is strongly statistically significant at $\alpha = 0.001$ level. For example in Fig. 3, since the coefficient of variance of the relationship is less than 1.0, it indicates that no erratic data points are present.

Waterflood Properties

Figure 5 is the residual oil saturation profiles at breakthrough and floodout for limestone cores. Breakthrough occurs when water is first produced at the outlet and floodout occurs at infinite water to oil ratio (or at a water to oil ratio of about 400:1, for the purpose of this study). The residual oil saturation versus irreducible water saturation at breakthrough and at floodout are plotted in Figs. 6 and 7. The irreducible water saturation is inversely related to residual oil saturation at breakthrough and at floodout.

Wettability Properties

From each of the waterflooded cores, 32 core plugs were extracted from along the flow path at an average interval of about 2.5 cm. The core plugs were perpendicular to the flood plane. During the process of the extraction, the distance of each core plug relative to the

inlet face of the core was noted. For a given distance, two core plugs were obtained, one from the bottom and the other from the top of the core. An average value of the wettability index is obtained for the two core plugs from a given distance. The distances are normalized by dividing the value of the measured distance relative to the core inlet by the total length of the core.

From the core plugs, an average value of wettability index was obtained for each of the cores. Based on these determinations, the limestone cores investigated in this study are classified as water-wet rocks. Figure 8 shows that average wettability index is inversely related to irreducible water saturation. The relationship is statistically significant at $\alpha = 0.1$ level. Figure 9 shows the plot of residual oil saturation versus average wettability index at floodout. They are directly related and the relationship is statistically significant at $\alpha = 0.05$ level. From this observation, it can be deduced that for water-wet limestone rocks, as wettability index increases, residual oil saturation at floodout also increases. At $\alpha = 0.1$ level, the relationship at breakthrough failed the statistical tests.

Mercury Porosimetry Properties

Similar to the analysis on the wettability data, average values of mercury porosimetry properties were obtained for each of the core samples from the core plugs. From the statistical description of the mercury porosimetry data, it is observed that the limestone rocks investigated are considered to be good reservoir rocks because they have both high mercury recovery efficiency and porosity values. According to Kopaska-Merkel and Friedman (1989), mercury recovery efficiency in mercury porosimetry is analogous to primary recovery of petroleum from natural reservoir, because both processes involve only simple pressure reduction. Hence, this type of rock with more than 25% mercury recovery efficiencies and fairly good mercury porosities, would perform well during primary oil recovery period.

Figure 10 shows a good relationship between total intrusion volume and mercury porosity, with a R^2 value of about 52% and high F-test statistic value of 15.31. Figure 11 shows that mercury recovery efficiency have an inverse relationship with the average pore diameter. The relationship is strong and statistically significant at $\alpha = 0.001$ level. Figure 12 shows that apparent (skeletal) density is directly related to total intrusion volume. The relationship between mercury recovery efficiency and porosity was found not to be statistically significant.

The agreement between porosity values obtained using mercury porosimetry and those obtained from the corefloods were not as good as was expected, as shown in Fig. 13. It was observed that if a 45° degree line is drawn on the plot, 11 of the data points lie above the line and the other 5 are close to the 45° line. This implies that the brine porosities are larger than the mercury measured porosities. According to Howard (1991), it is expected that the porosity measured by mercury porosity would be less than the porosity measured by coreflood methods, because of the limited intrusion pressures employed. The relationship of brine permeability versus total intrusion volume is presented in Fig. 14.

Figure 15 presents the capillary-pressure versus cumulative mercury intrusion/extrusion curve for plug 28 of sample core 15B. The term capillary-pressure, as used in the reservoir analysis literature and in this paper, refers to the injection pressure necessary to inject non-wetting fluids (such as mercury) into the pore spaces of a rock. The mode type of the curve is bimodal with gently-sloping shape. This is further confirmed in Fig. 16, which is the plot of capillary pressure versus incremental mercury intrusion/extrusion curve for the same plug. For most of the limestone core plugs investigated in this study, bimodal gently-sloping shape capillary-pressure curves were common.

EMPIRICAL MODELS

Empirical models have been developed which relate residual oil saturation with rock-pore characteristics. The models are given at two periods: at breakthrough and at floodout. Multiple regression analysis, which is one of the most widely used statistical tools was employed for the development of the models. On the basis of these analyses, the dependent variables, residual oil saturation at both the breakthrough and floodout periods, could be best represented as a function of the independent variables in linear terms or a minimum amount of interactions among the variables, as are later presented in Eqs. 2 and 3, respectively. The best subsets algorithms "BREG", which is available in MINITAB statistical computer package (Ryan et al.), was utilized. They are time-saving algorithms and they allow the best subsets according to a specified criteria to be identified, without requiring the fitting of all of the possible subset regression models.

Residual Oil Saturation At Breakthrough

The output for the best subsets algorithms for the development of the model for the residual oil saturation at breakthrough is shown in Table 3. In this table and in Table 4, the asterisk on one of the number of independent variables, shows the best subsets chosen, considering the selection criteria. The final model developed for the predictions of limestones residual oil saturation at breakthrough is given as:

$$S_{or_{@BT}} = 9.361 - 48.04\,\phi + 5.768\,\tau - 0.879\,F - 1.003\,S_{wi} - 0.640\,\rho_s + 1.098\,RE \qquad (2)$$

The R^2 for Eq. 2 is 90.4%, its adj.-R^2 is 84.1%, its C_p criterion value is 3.1 and its standard deviation is 0.029. The model's F-test statistic value is 14.18 and the p-value is 0.000, which implies that the model is statistically significant at $\alpha = 0.001$ level. Since the best subset chosen for this equation contains 6 independent variables, the number of parameters, p, is therefore equal to 7 (which is the number of independent variables plus the constant term included in Eq. 2). This implies that since the developed model has C_p less than p, the model is unbiased.

Residual Oil Saturation At Floodout

The output for the best subsets algorithms for the development of the model for the residual oil saturation at floodout is shown in Table 4. The final model developed for the predictions of limestones residual oil saturation at floodout is given as:

$$S_{or_{@FO}} = 0.887 - 0.00561\ k - 0.00897\ F + 0.115WI - 0.461\ S_{wi} - 4.123\ V_{int.} - 0.209\ RE \quad (3)$$

The R^2 for Eq. 3 is 94.4%, its adj.-R^2 is 90.7%, its C_p criterion value is 2.2 and its standard deviation is 0.014. The model's F-test statistic value is 10.84 and the p-value is 0.001, which implies that the model is statistically significant at $\alpha = 0.001$ level. The developed model contains 6 independent variables, which implies that the model is unbiased.

CONCLUSIONS

The following conclusions are deduced from this study:

1. The limestone cores investigated are all water-wet, and their average wettability indices have direct relationships with residual oil saturations.

2. Mercury recovery efficiencies exhibited inverse relationships with the average pore diameters for limestones.

3. The limestone cores investigated were all found to exhibit bimodal gentle-sloping shape capillary-pressure curves.

4. Limestones porosity, permeability, tortuosity, formation resistivity factor, irreducible water saturation, wettability, and mercury porosimetry properties can be empirically related to their residual oil saturations at breakthrough and at floodout.

NOMENCLATURE

Adj. R-sq.	=	adjusted coefficient of determination
B.T.	=	breakthrough time
C_p	=	C_p criterion
C.V.	=	coefficient of variation
$\overline{D}$	=	average pore diameter (micrometer)
F	=	formation resistivity factor
F	=	statistical F-test
F.O.	=	floodout time
k	=	absolute permeability (md)
$Lu_w\mu_w$	=	scaling coefficient
n	=	number of samples
R	=	correlation coefficient
R^2	=	coefficient of determination
R-sq.	=	coefficient of determination
RE	=	mercury recovery efficiency (fraction)
S_{or}	=	residual oil saturation (fraction)
S_s	=	specific surface area (cm^2/cm^3)
S_{wi}	=	irreducible water saturation (fraction)
SA	=	total pore area or surface area (m^2/g)
u_w	=	flood rate/unit volume (cm/min)
$V_{int.}$	=	total intrusion volume or pore volume (ml/g)
WI	=	wettability index
α	=	level of significance
μ_w	=	water viscosity (cp)
ρ_s	=	apparent (skeletal) density (g/ml)
σ	=	standard deviation
τ	=	tortuosity
ϕ	=	porosity (fraction)
ϕ_{Hg}	=	mercury porosimetry porosity (fraction)

ACKNOWLEDGEMENTS

The authors wish to acknowledge the financial support of the U.S. Department of Energy to The Pennsylvania State University through Contract No. DE-AC22-89BC14477.

REFERENCES

Amott, E.: "Observations Relating to the Wettability of Porous Rock," *AIME Trans.*, (1959), **216,** 156-162.

Amyx, J.W., Bass, D.M. Jr., and Whiting, R.L.: Petroleum Reservoir Engineering, 610 pp., McGraw-Hill Book Co., New York, NY., 1960.

Anderson, W.G.: "Wettability Literature Survey - Part 2: Wettability Measurement," *JPT*, (Nov. 1986), 1246-1262.

Cuiec, L.: "Wettability and Oil Reservoirs," *North Sea Oil & Gas Reservoir*, The Norwegian Inst. of Tech., (Graham and Trotman, 1987), 193-207.

Ghosh, S.K., and Friedman, G.M.: "Petrophysics of a Dolostone Reservoir: San Andres Formation (Permian), West Texas," *Carbonates and Evaporites*, (1989), **4,** No. 1, 45-117.

Howard, J.J.: "Porosimetry Measurement of Shale Fabric and its Relationship to Illite/Smectite Diagenesis," *The Clays and Clay Minerals*, (1991), **39,** No. 4, 355-361.

Kopaska-Merkel, D.C., and Friedman, G.M.: "Petrofacies Analysis of Carbonate Rocks: Example from Lower Paleozoic Hunton Group of Oklahoma and Texas," *AAPG Bull.*, (Nov. 1989), **73,** No. 11, 1289-1306.

Neter, J., Wasserman, W., and Kutner, M.H.: Applied Linear Statistical Models, 1181 pp., 3rd. Ed., Irwin, Boston, MA., 1990.

Owolabi, O.O.: "Relating Uncommon Rock/Fluid Properties to Oil Recovery for Various Types of Oil Bearing Rocks: Experimental and Empirical Studies," Ph.D. Thesis, The Pennsylvania State University, University Park, PA., May 1993.

Ryan, B.F., Joiner, B.L., and Ryan, T.A. Jr.: Minitab Handbook, 379 pp., 2nd. Ed., Duxbury Press, Boston, MA., 1985.

Table 1: Physical Properties of the Oil and Brine

Oil Density @ 35°C (gm/cc)	0.83
Brine Density @ 35°C (gm/cc)	1.01
Oil Viscosity @ 35°C (cp)	10.00
Brine Viscosity @ 35°C (cp)	1.00
Interfacial Tension (dynes/cm)	26.33

Table 2: Physical and Petrophysical Properties of the Limestone Cores

Core No.	Length (cm)	Dia. (cm)	Inj. Rate (cc/min)	Scaling Coeff., $L\mu_o/\mu_w$	Core Pore Vol. (cc)	Brine Porosity (%)	Absolute Perm. (md)	Pore Vol. Inj. (cc)	H.C. Pore Vol. (cc)	Cap. Number, N^*_{ca} (E-05)
9A	45.64	3.78	1.23	5.00	82.75	16.16	19.83	2.18	49.5	6.94
9B	45.16	3.76	1.23	5.00	80.37	16.03	18.10	1.36	43.9	7.01
10A	45.32	3.77	1.24	5.04	78.28	15.48	14.99	1.62	48.5	7.02
10B	45.08	3.77	1.25	5.03	78.54	15.56	14.51	2.25	37.7	7.07
11A	45.24	3.87	1.31	5.03	84.46	15.84	9.70	1.57	48.9	7.04
11B	45.24	3.89	1.32	5.03	83.08	15.48	8.47	1.71	46.5	7.04
12A	45.48	3.83	1.27	5.00	77.81	14.81	10.51	2.41	40.3	6.96
12B	45.24	3.83	1.28	5.03	75.82	14.55	14.23	2.42	41.6	7.03
13A	45.24	3.81	1.27	5.03	77.51	14.99	16.31	1.84	35.3	7.03
13B	45.32	3.81	1.27	5.03	77.78	15.01	11.09	2.44	47.4	7.03
14A	45.40	3.84	1.28	5.01	74.39	14.13	10.09	2.48	44.6	6.99
14B	45.08	3.83	1.28	5.01	74.10	14.28	11.20	2.49	42.1	7.04
15A	45.72	3.79	1.24	5.02	75.74	14.68	12.30	2.40	41.7	6.95
15B	44.93	3.80	1.25	4.96	77.60	15.25	10.92	2.49	48.8	6.99
16A	45.56	3.86	1.29	5.02	80.57	15.10	10.48	2.13	41.9	6.97
16B	40.00	3.88	1.48	5.00	69.96	14.77	9.12	3.42	39.4	7.91

Table 3: Best Subsets Regression for Residual Oil Saturation at Breakthrough for Limestones

Vars.	R-sq	Adj. R-sq	C_p	σ	ϕ	k	τ	F	WI	S_{wi}	V_{mic}	SA	S_s	$\bar{D}$	ρ_s	RE
1	48.5	44.8	15.2	0.054		x										
1	43.7	39.7	17.7	0.057							x					
2	70.8	66.3	5.4	0.043		x				x						
2	69.6	65.0	6.0	0.043						x						x
3	62.8	58.4	11.1	0.034						x					x	x
3	60.5	55.6	12.3	0.036		x				x				x		
4	84.3	78.5	2.3	0.034	x					x					x	x
4	84.2	78.4	2.3	0.034		x				x					x	x
5	88.2	82.3	2.2	0.031	x		x	x		x						x
5	85.4	78.2	3.7	0.034	x			x		x					x	x
6*	90.4	84.1	3.1	0.029	x		x	x		x					x	x
6	88.9	81.6	3.8	0.031	x		x	x		x		x				x
7	90.8	82.7	4.9	0.030	x	x	x	x		x					x	x
7	90.5	82.1	5.0	0.031	x		x	x	x	x					x	x
8	91.2	81.1	6.6	0.032	x	x	x	x	x	x					x	x
8	91.1	80.9	6.7	0.032	x	x	x	x		x			x		x	x
9	91.9	79.9	8.3	0.033	x	x	x	x	x	x				x	x	x
9	91.3	78.3	8.6	0.034	x	x	x	x	x	x			x		x	x
10	92.6	77.9	9.9	0.034	x		x	x		x	x	x	x	x	x	x
10	92.0	76.1	10.2	0.036	x	x	x	x	x	x	x			x	x	x
11	94.0	77.3	11.2	0.034	x	x	x	x		x	x	x	x	x	x	x
11	92.7	72.8	11.8	0.038	x		x	x	x	x	x	x	x	x	x	x
12	94.3	71.6	13.0	0.039	x	x	x	x	x	x	x	x	x	x	x	x

Table 4: Best Subsets Regression for Residual Oil Saturation at Floodout for Limestones

Vars.	R-sq	Adj. R-sq	C_p	σ	ϕ	k	τ	F	WI	S_{wi}	V_{mic}	SA	S_s	$\bar{D}$	ρ_s	RE
1	64.0	61.5	15.2	0.029						x						
1	40.9	36.7	32.8	0.037							x					
2	84.6	82.3	1.6	0.0120		x				x						
2	76.8	73.2	7.6	0.024						x	x					
3	88.2	85.2	1.0	0.018		x				x		x				
3	87.0	83.7	1.9	0.019		x			x	x						
4	91.7	88.6	0.3	0.016		x			x	x	x					
4	89.9	86.2	1.7	0.017		x			x	x		x				
5	93.4	90.0	1.0	0.015		x			x	x	x					x
5	93.3	90.0	1.1	0.015		x	x		x	x	x					
6*	94.4	90.7	2.2	0.014		x		x	x	x	x				x	
6	94.2	90.4	2.4	0.015		x	x		x	x	x					x
7	94.8	90.3	3.9	0.015	x	x	x	x	x	x	x					
7	94.7	90.0	4.0	0.015		x		x	x	x	x				x	x
8	95.2	89.6	5.7	0.015	x	x	x	x	x	x	x					x
8	95.1	89.5	5.7	0.015	x	x	x	x	x	x	x				x	
9	95.5	88.8	7.4	0.016	x		x	x	x	x	x	x	x		x	
9	95.4	88.4	7.5	0.016	x	x	x	x	x	x		x	x			x
10	95.8	87.3	9.2	0.017	x	x	x	x	x	x		x	x		x	x
10	95.6	86.9	9.3	0.017	x	x	x	x	x	x	x		x		x	x
11	96.0	84.9	11.0	0.019	x	x	x	x	x	x	x	x	x	x		x
11	95.9	84.7	11.1	0.018	x	x	x	x	x	x	x	x	x		x	x
12	96.0	80.2	13.0	0.021	x	x	x	x	x	x	x	x	x	x	x	x

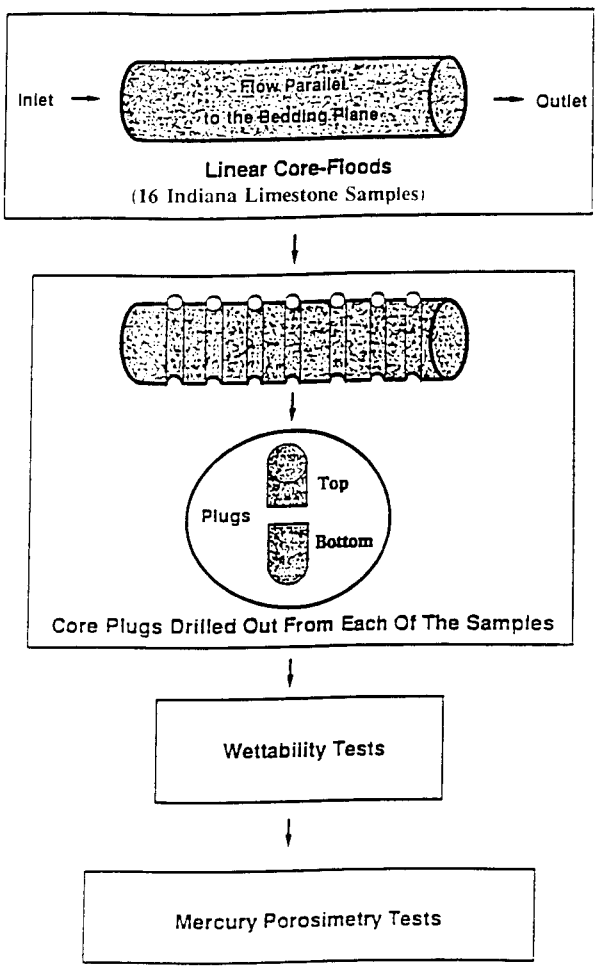

Fig. 1: Schematic of the Experimental Procedure.

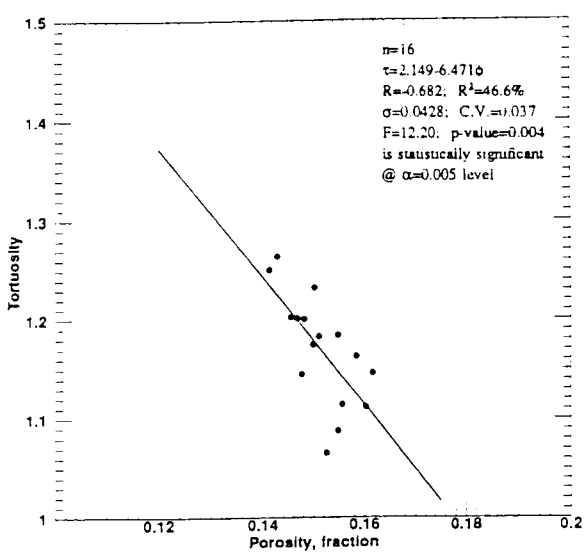

Fig. 3: Tortuosity vs. Porosity for Limestone Cores.

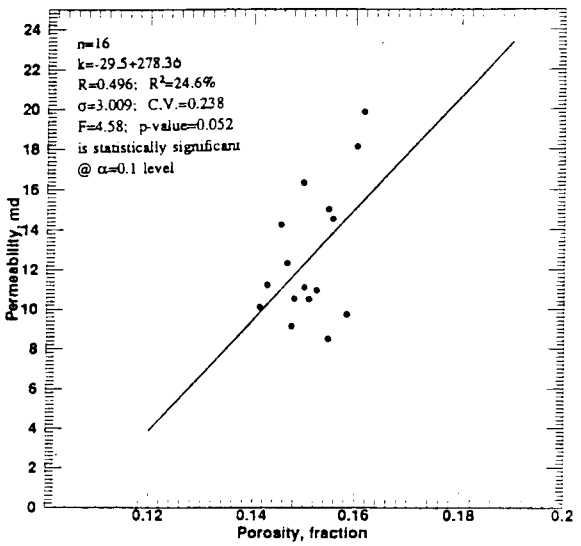

Fig. 2: Permeability vs. Porosity for Limestone Cores.

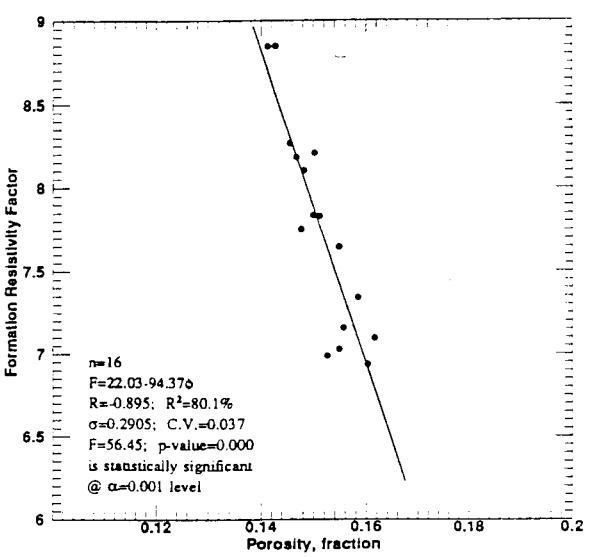

Fig. 4: Formation Resistivity Factor vs. Porosity for Limestone Cores.

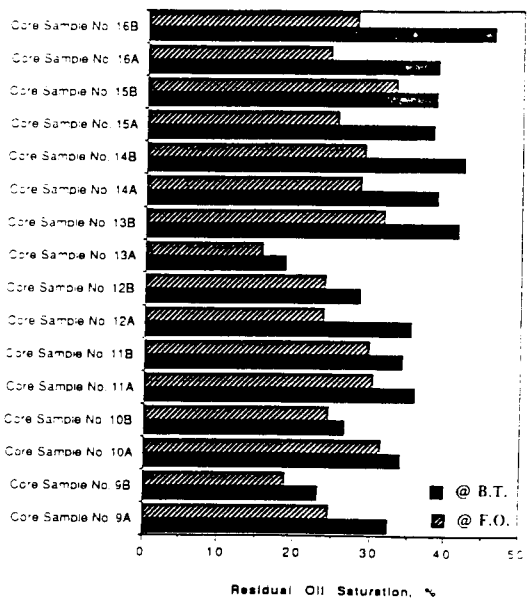

Fig. 5: Residual Oil Saturation Profiles at Breakthrough and Floodout for Limestone Cores.

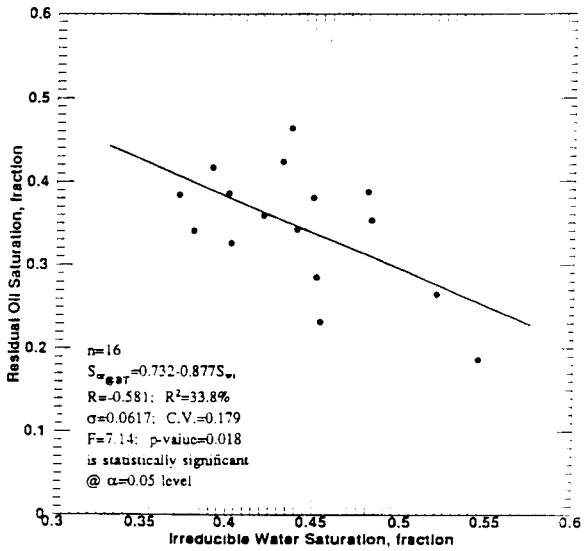

Fig. 6: Residual Oil Saturation vs. Irreducible Water Saturation for Limestone Cores at Breakthrough.

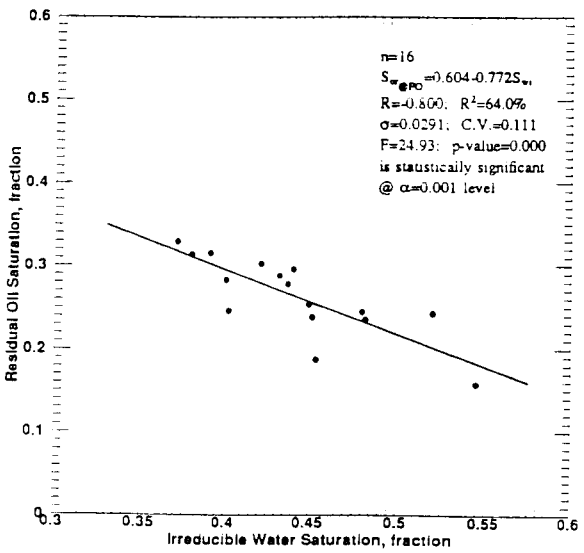

Fig. 7: Residual Oil Saturation vs. Irreducible Water Saturation for Limestone Cores at Floodout.

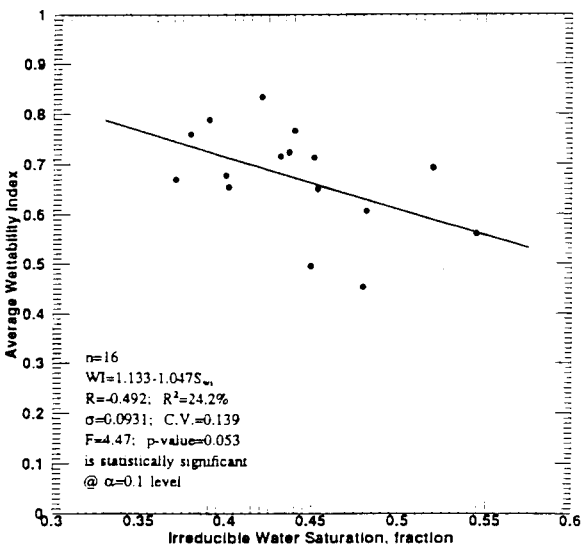

Fig. 8: Average Wettability Index vs. Irreducible Water Saturation for Limestone Cores.

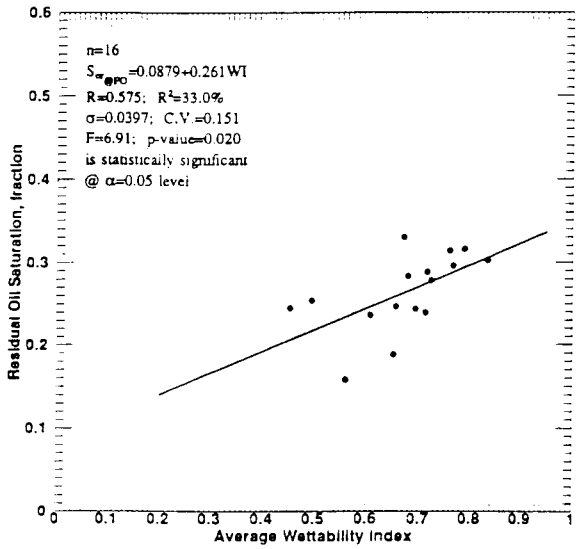

Fig. 9: Residual Oil Saturation vs. Average Wettability Index for Limestone Cores at Floodout.

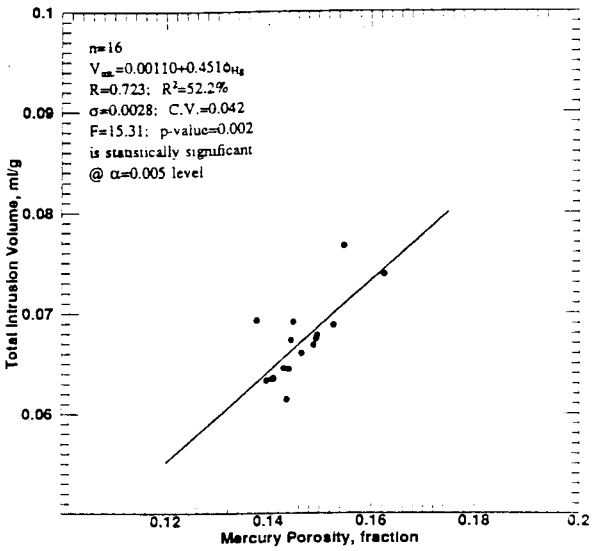

Fig. 10: Total Intrusion Volume vs. Mercury Porosity for Limestone Cores.

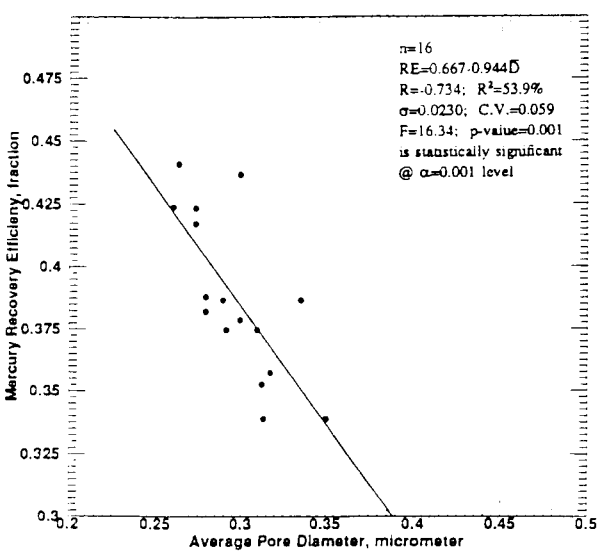

Fig. 11: Recovery Efficiency vs. Pore Diameter for Limestone Cores.

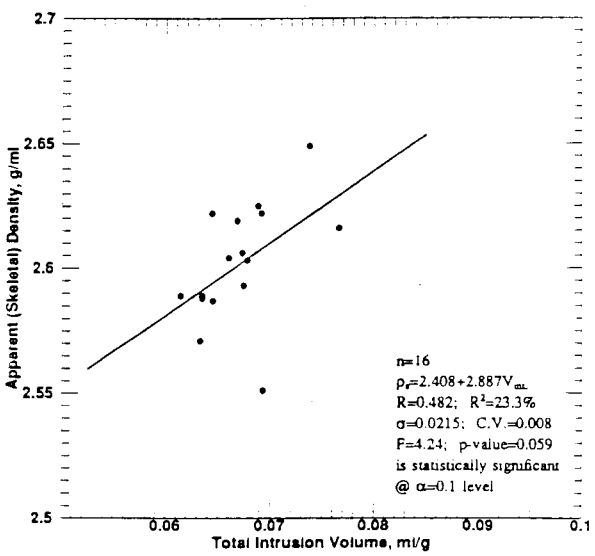

Fig. 12: Skeletal Density vs. Total Intrusion Volume for Limestone Cores.

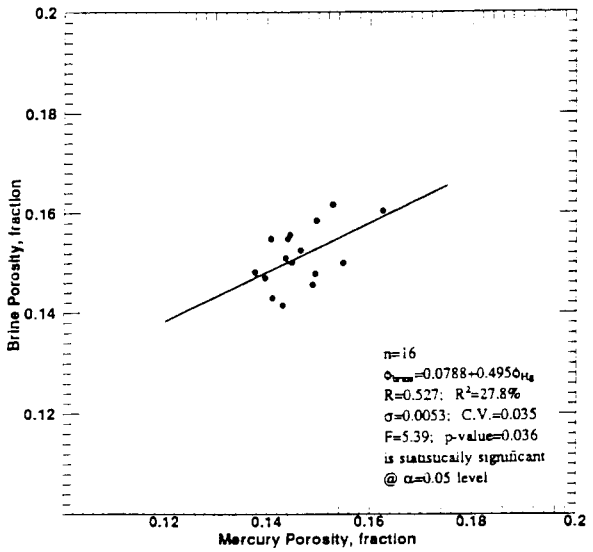

Fig. 13: Brine Porosity vs. Mercury Porosity for Limestone Cores.

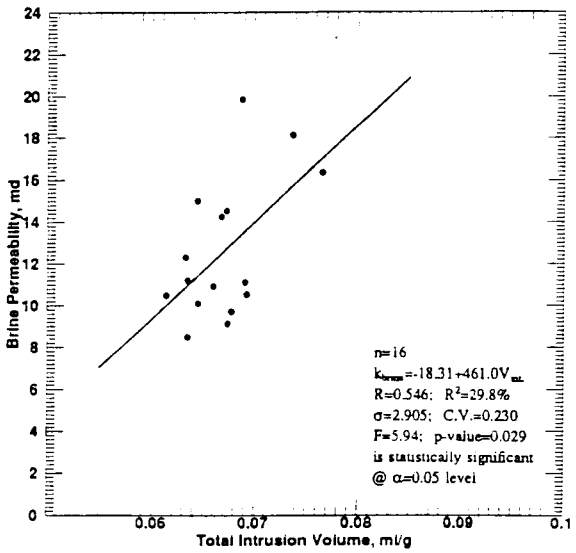

Fig. 14: Brine Permeability vs. Total Intrusion Volume for Limestone Cores.

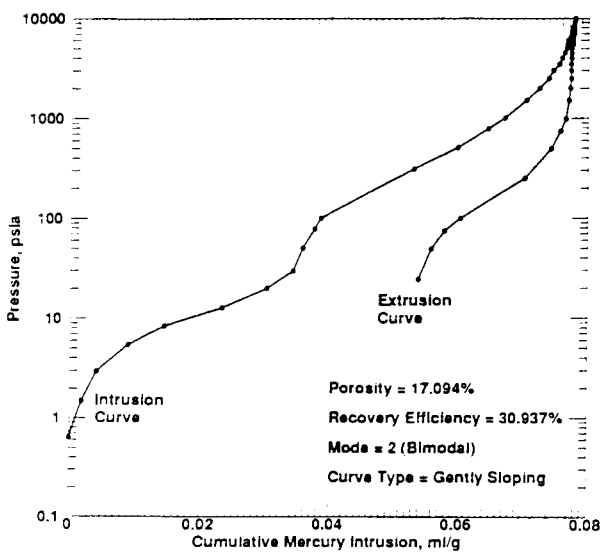

Fig. 15: Capillary Pressure vs. Cumulative Mercury Intrusion Curve for Limestone Core 15B - Plug 28.

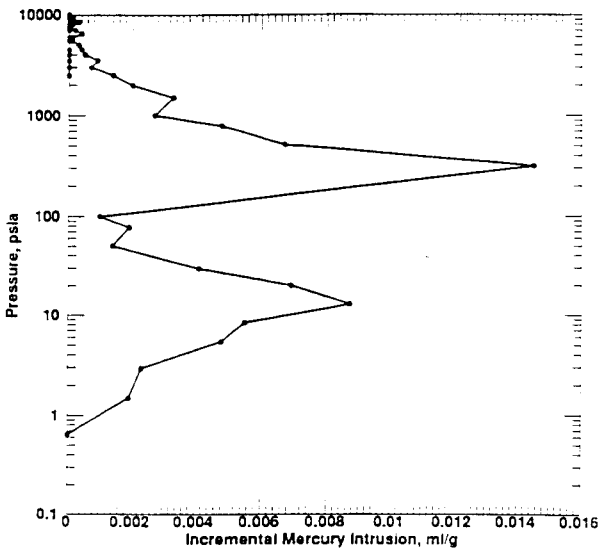

Fig. 16: Capillary Pressure vs. Incremental Mercury Intrusion Curve for Limestone Core 15B - Plug 28.